Thermodynamic and Energy Efficiency Analysis of Power Generation from Natural Salinity Gradients by Pressure Retarded Osmosis

ARTICLE *in* ENVIRONMENTAL SCIENCE & TECHNOLOGY · APRIL 2012

Impact Factor: 5.33 · DOI: 10.1021/es300060m · Source: PubMed

2 AUTHORS, INCLUDING:

Menachem Elimelech
Yale University
394 PUBLICATIONS **32,554** CITATIONS

Environmental Science & Technology

Article

pubs.acs.org/est

Thermodynamic and Energy Efficiency Analysis of Power Generation from Natural Salinity Gradients by Pressure Retarded Osmosis

Ngai Yin Yip and Menachem Elimelech*

Department of Chemical and Environmental Engineering, Yale University, New Haven, Connecticut 06520-8286, United States

Supporting Information

ABSTRACT: The Gibbs free energy of mixing dissipated when fresh river water flows into the sea can be harnessed for sustainable power generation. Pressure retarded osmosis (PRO) is one of the methods proposed to generate power from natural salinity gradients. In this study, we carry out a thermodynamic and energy efficiency analysis of PRO work extraction. First, we present a reversible thermodynamic model for PRO and verify that the theoretical maximum extractable work in a reversible PRO process is identical to the Gibbs free energy of mixing. Work extraction in an irreversible constant-pressure PRO process is then examined. We derive an expression for the maximum extractable work in a constant-pressure PRO process and show that it is less than the ideal work (i.e., Gibbs free energy of mixing) due to inefficiencies intrinsic to the process. These inherent inefficiencies are attributed to (i) frictional losses required to overcome hydraulic resistance and drive water permeation and (ii) unutilized energy due to the discontinuation of water permeation when the osmotic pressure difference becomes equal to the applied hydraulic pressure. The highest extractable work in constant-pressure PRO with a seawater draw solution and river water feed solution is 0.75 kWh/m^3 while the free energy of mixing is 0.81 kWh/m^3—a thermodynamic extraction efficiency of 91.1%. Our analysis further reveals that the operational objective to achieve high power density in a practical PRO process is inconsistent with the goal of maximum energy extraction. This study demonstrates thermodynamic and energetic approaches for PRO and offers insights on actual energy accessible for utilization in PRO power generation through salinity gradients.

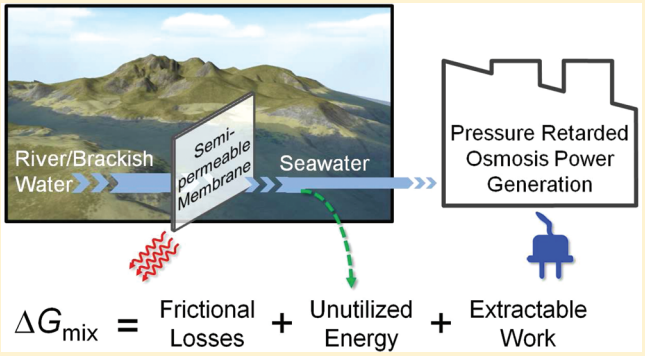

INTRODUCTION

The impetus to reduce greenhouse gas emissions and mitigate climate change has invigorated research on alternative power sources.[1] Natural salinity gradients have been identified as a promising source of clean renewable energy. The free energy of mixing that is released when two solutions of different salt concentration are combined can be harnessed for sustainable power production.[2] When fresh river water mixes with the sea, free energy equal to a 270 m high waterfall is released.[3] The annual global river discharge of ~37 300 km^3 represents an enormous source of renewable energy[4] that can potentially produce an estimated 2 TW of electricity, or 13% of global electricity consumption.[5]

Several methods have been proposed to harvest this sustainable energy source, including reverse electrodialysis,[6,7] mixing entropy batteries,[5] and pressure retarded osmosis (PRO).[8,9] In PRO salinity power generation, the osmotic pressure difference across a semipermeable membrane drives the permeation of water from the dilute river water "feed solution" into concentrated seawater "draw solution". A hydraulic pressure less than the osmotic pressure difference is applied to the draw solution, thereby "retarding" water flux across the membrane, and a hydroturbine extracts work from the expanding draw solution volume. In 2009, the world's first PRO power plant came into operation in Norway, demonstrating the potential viability of the process.[9] The prospects of cost-effective osmotic power production are further bolstered by the recent development of thin-film composite PRO membranes with transport and structural properties projected to produce high power densities.[10−12]

Previous studies on power generation from natural salinity gradients employed the Gibbs free energy of mixing to evaluate the realizable energy.[3,5,13,14] However, the free energy of mixing represents the theoretical maximum energy that is available for useful work by a reversible thermodynamic process and does not take into account the intrinsic thermodynamic inefficiencies. Hence, actual work output will always be less than the theoretical energy available because practical work extraction processes are irreversible in nature and, thus, generate entropy.[15−17] To obtain the actual extractable work—a more applicable and relevant figure—thermodynamic conversion efficiencies have to be incorporated into the energy analysis.

Received: January 10, 2012
Revised: March 28, 2012
Accepted: April 1, 2012
Published: April 2, 2012

   dx.doi.org/10.1021/es300060m | Environ. Sci. Technol. 2012, 46, 5230−5239

In this study we carry out a thermodynamic and energy efficiency analysis of pressure retarded osmosis. The theoretical maximum extractable work in a PRO process is determined from a reversible thermodynamic model for PRO and compared to the Gibbs free energy of mixing. We then examine the thermodynamic efficiency of work extraction in a practical constant-pressure PRO process using natural salinity gradients. The inherent inefficiencies of frictional losses and unutilized energy imposed by the constant-pressure PRO process are analyzed and discussed. Finally, we look at the practical constraints of an actual PRO process and highlight the implications on energy extraction efficiency. Our analysis of the thermodynamic considerations in the extraction of work from natural salinity gradients provides insights into the energy efficiency intrinsic to the PRO power generation process.

■ ENERGY OF MIXING

When two solutions of different compositions are mixed, the Gibbs free energy of mixing is released. In this section we draw upon established thermodynamic concepts[15,16,18−20] to present a condensed theoretical background on the energy change of mixing for a binary system of aqueous strong electrolyte solutions. A detailed presentation of the energy change of mixing can be found in the Supporting Information (SI).

Mixing Releases Free Energy. Mixing two solutions, A and B, of different composition yields a resultant mixture, M. The difference in the Gibbs free energy between the final mixture (G_M) and initial (G_A and G_B) solutions gives the change in free energy of mixing.[15] The Gibbs free energy of mixing per mole of the system, ΔG_{mix}, is[16]

$$-\Delta G_{mix} = RT\left\{\left[\sum x_i \ln(\gamma_i x_i)\right]_M - \phi_A\left[\sum x_i \ln(\gamma_i x_i)\right]_A - \phi_B\left[\sum x_i \ln(\gamma_i x_i)\right]_B\right\} \quad (1)$$

where x_i is the mole fraction of species i in solution, R is the gas constant, and T is temperature. The activity coefficient, γ_i, is incorporated to account for the behavior of nonideal solutions, and is a function of the temperature, pressure, and solution composition.[16] ϕ_A and ϕ_B are the ratios of the total moles in solutions A or B, respectively, to the total moles in the system (i.e., $\phi_A + \phi_B = 1$). Here, we adopt the negative convention for the energy of mixing to reflect that energy is released.

An inspection of eq 1 reveals that ΔG_{mix} is dependent on the relative proportion of the initial solutions (ϕ_A and ϕ_B) and the composition of the solutions (x_i and, implicitly, γ_i) for a mixing process at constant temperature and pressure. The Gibbs free energy of mixing described in eq 1 is applicable for all general mixing processes,[15] and it is equal and opposite in sign to the minimum energy required to separate the mixture M into products A and B.[19]

Energy Change of Mixing for Strong Electrolyte Solutions. For a two-component system of aqueous strong electrolyte solutions, the two species are water and a salt that dissociates completely in solution (denoted by subscripts w and s, respectively). For relatively low salt concentration solutions, both the mole fraction of water, x_w, and the activity coefficient, γ_w, can be approximated to unity.[18] Therefore, $\ln(\gamma_w x_w)$ for the initial solutions and final mixture approaches zero in eq 1. In this case, the contribution of the salt species to ΔG_{mix} overwhelms the contribution of the water species, and the molar Gibbs free energy of mixing (eq 1) simplifies to

$$-\frac{\Delta G_{mix}}{\nu RT} \approx \left[x_s \ln(\gamma_s x_s)\right]_M - \phi_A\left[x_s \ln(\gamma_s x_s)\right]_A - \phi_B\left[x_s \ln(\gamma_s x_s)\right]_B \quad (2)$$

where ν, the number of ions each electrolyte molecule dissociates into, accounts for the multiple ionic species contribution of the strong electrolyte salt.[16]

For practicality and ease of application, the mole fraction and molar mixing energy in eq 2 are converted to molar salt concentration and Gibbs free energy of mixing per unit volume, respectively. This is achieved by assuming the volumetric and mole contribution of the salt to the solution is negligible compared to water, and that the volume of the system remains constant in the mixing process ($V_A + V_B = V_M$). Thus, the mole fractions can be approximated to the volumetric fractions. The detailed steps of the conversion can be found in the SI. The Gibbs free energy of mixing per unit volume of the resultant mixture, $\Delta G_{mix,V_M}$, is then

$$-\frac{\Delta G_{mix,V_M}}{\nu RT} \approx c_M \ln(\gamma_{s,M} c_M) - \phi c_A \ln(\gamma_{s,A} c_A) - (1-\phi) c_B \ln(\gamma_{s,B} c_B) \quad (3)$$

where c is the molar salt concentration of the aqueous solutions and ϕ is the ratio of the total moles in solution A to the total moles in the system (i.e., $\phi = \phi_A$ and $1 - \phi = \phi_B$). Based on the above simplifying assumptions, ϕ is also the volumetric ratio of solution A to the total system volume (i.e., $\phi = V_A/V_M$). An examination of eq 3 shows that $\Delta G_{mix,V_M}$ is solely a function of the salt concentration and mole fraction (or volume fraction) of the initial solutions (c_M is determined by c_A, c_B, and ϕ, while γ is dependent on c).

In power generation from natural salinity gradients, often seawater from the ocean is abundant while fresh water from the estuaries is the limiting resource. As such, expressing the mixing energy per unit volume of the dilute solution would more accurately capture the energy available for extraction. Multiplying eq 3 by V_M/V_A ($\approx 1/\phi$) yields the Gibbs free energy of mixing per unit volume of A (the more dilute solution):

$$-\frac{\Delta G_{mix,V_A}}{\nu RT} \approx \frac{c_M}{\phi}\ln(\gamma_{s,M} c_M) - c_A \ln(\gamma_{s,A} c_A) - \frac{(1-\phi)}{\phi} c_B \ln(\gamma_{s,B} c_B) \quad (4)$$

Figure 1 shows $\Delta G_{mix,V_A}$, calculated using eq 4, for the mixing of a fresh water source with seawater as a function of the mole fraction of the fresh water, ϕ, in 0.1 increments. Fresh waters (dilute solution A) with salinities of 1.5 and 17 mM (~88 and ~1000 mg/L) NaCl were selected to represent river water (blue square symbols) and brackish water (red circle symbols), respectively.[10] The seawater (concentrated solution B) was taken to be 600 mM (35 g/L) NaCl[10] and the temperature, T, was fixed at 298 K. The calculated values are presented in SI Table S1. The activity coefficients of the initial solutions (A and B) and resultant mixture (M) were approximated by linear interpolation of the data in SI Table S2.

The highest mixing energy of 0.77 kWh/m^3 (2.76 kJ/L) is achieved for river water when ϕ tends to zero (i.e., an infinitesimal amount of fresh water mixes with an infinitely large volume of seawater). This value of 0.77 kWh/m^3 is similar to

dx.doi.org/10.1021/es300060m | Environ. Sci. Technol. 2012, 46, 5230−5239

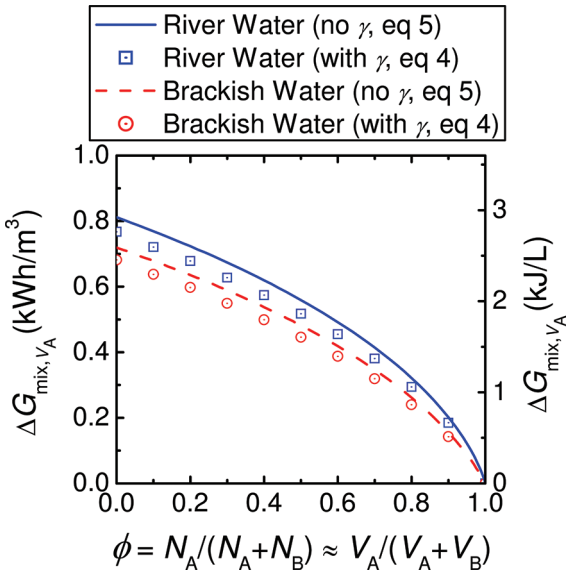

Figure 1. Gibbs free energy of mixing, $\Delta G_{mix,V_A}$, as a function of the mole fraction of the fresh river or brackish water (A) to both the fresh water and seawater (A and B), ϕ. The change in free energy of mixing is expressed as the energy released per unit volume of the river or brackish water. Blue square symbols and red circle symbols indicate $\Delta G_{mix,V_A}$ calculated with activity coefficients (eq 4) for river water and brackish water, respectively. Solid blue line and dashed red line represent $\Delta G_{mix,V_A}$ determined without γ (eq 5) for river water and brackish water, respectively. The calculations were carried out for a temperature of 298 K, and the concentration of seawater was assumed to be 600 mM (35 g/L) NaCl, while the concentrations of river water and brackish water were taken to be 1.5 and 17 mM (88 and 1000 mg/L) NaCl, respectively. For the dilute concentrations considered here, the mole fraction can be approximated to be the volumetric fraction of freshwater.

the minimum energy to desalinate seawater at 0% recovery[21,22] (the minor difference between the values is attributed to the slight difference in concentrations and approximations employed for the calculations). This observation is consistent with our understanding of reversible thermodynamics: the separation energy at 0% recovery is equal in magnitude but opposite in sign to the free energy of mixing at $\phi = 0$. As the mole fraction of the fresh water increases, $\Delta G_{mix,V_A}$ decreases and eventually reaches zero at $\phi = 1$. A similar trend is observed for brackish water, except that at $\phi = 0$, the energy of mixing is 0.68 kWh/m^3 (2.45 kJ/L). This value is lower compared to river water due to the higher initial salt content of brackish water. Note that actual seawater contains a mixed composition of ionic species other than Na^+ and Cl^-,[23] and the energy of mixing will, therefore, differ slightly from the above calculated values.

ΔG_{mix} for Ideal Solutions. For the relatively low salt concentrations investigated in this study, the mole fraction of salt (or molar salt concentration) dominates over the salt activity coefficient in the logarithmic term in eq 4, i.e., $\ln(\gamma_s x_s) = \ln(\gamma_s) + \ln(x_s) \approx \ln(x_s)$. For example, for a 600 mM NaCl solution, which is representative of seawater, $\ln(x_s) = \ln(0.0107) = -4.54$ is much greater in magnitude than $\ln(\gamma_s) = \ln(0.672) = -0.40$ (SI Table S2).[18] To further simplify the analysis, we can neglect the activity coefficients (i.e., assume ideal behavior) and eq 4 further reduces to

$$-\frac{\Delta G_{mix,V_A}}{\nu RT} \approx \frac{c_M}{\phi}\ln c_M - c_A \ln c_A - \frac{(1-\phi)}{\phi} c_B \ln c_B \qquad (5)$$

Figure 1 shows $\Delta G_{mix,V_A}$, determined using eq 5, for the mixing of a river water (solid blue line) and brackish water (dashed red line) with seawater, as a function of ϕ. The $\Delta G_{mix,V_A}$ values calculated using eq 5 for 0.1 increments in ϕ are presented in SI Table S1. The concentrations of the fresh water sources and seawater were the same as those used in the previous calculations of $\Delta G_{mix,V_A}$ (i.e., with eq 4). The highest mixing energies of 0.81 kWh/m^3 (2.92 kJ/L) and 0.72 kWh/m^3 (2.59 kJ/L) are achieved for river water and brackish water, respectively, when ϕ tends to zero. The free energy of mixing determined without the activity coefficient, γ, exhibits a similar trend compared to $\Delta G_{mix,V_A}$ with γ (i.e., eq 4), except the values are slightly higher (~5.4–9.3%, SI Table S1). The similar trend and magnitude of the mixing energies between eqs 4 and 5 reinforces the validity of the simplifying step to ignore the activity coefficients. Although some precision is sacrificed, eq 5 offers a great ease of application, compared to eq 4, as $\Delta G_{mix,V_A}$ can be determined directly.

The change in Gibbs free energy represents an upper bound on the energy that can be extracted for useful work, regardless of the pathway. However, the second law of thermodynamics stipulates that in actual cases, the useful work extracted is always less than $\Delta G_{mix,V_A}$ due to the production of entropy.[15] The inherent irreversible energy losses in the work extraction processes are analogous to the thermodynamic inefficiencies of separation processes, where the energy consumed to carry out the purification is always greater than the theoretical minimum energy of separation.[19] Therefore, an efficient work extraction process is one that minimizes such thermodynamic inefficiencies and utilizes most of the available energy.

REVERSIBLE THERMODYNAMIC MODEL OF PRESSURE RETARDED OSMOSIS

In pressure retarded osmosis power generation, a semipermeable membrane separates two solutions of different concentration. The osmotic pressure difference that develops across the membrane drives the permeation of water from the dilute feed solution into the more concentrated draw solution. A hydraulic pressure less than the osmotic pressure difference is applied to the draw solution and a hydroturbine extracts work from the expanding draw solution volume. In this section, we present a reversible thermodynamic model of PRO and show the derivation of the theoretical maximum extractable work. In the following analyses, a 600 mM NaCl draw solution is used to simulate seawater of ~35 g/L TDS, while the salt concentrations of the feed solutions are 1.5 and 17 mM NaCl, to represent river water and brackish water of approximately 88 and 1000 mg/L TDS, respectively.[10] The temperature is 298 K and assumed to remain constant throughout the PRO process.

Pressure Retarded Osmosis Model. Figure 2 shows the schematics of a PRO process. The dilute feed solution (of initial concentration c_F^0 and volume V_F^0) is separated from the draw solution (of initial concentration c_D^0 and volume V_D^0) by an ideal semipermeable membrane that completely rejects salt (NaCl) while allowing water to permeate (Figure 2A). We assume the van't Hoff relation to be valid (i.e., ideal solutions) for the concentration range considered here. Therefore, the osmotic pressure of the solutions is $\pi = \nu cRT$, where ν is the number of ionic species each salt molecule dissociates into, c is the molar salt concentration, R is the gas constant, and T is the absolute temperature.

dx.doi.org/10.1021/es300060m | Environ. Sci. Technol. 2012, 46, 5230–5239

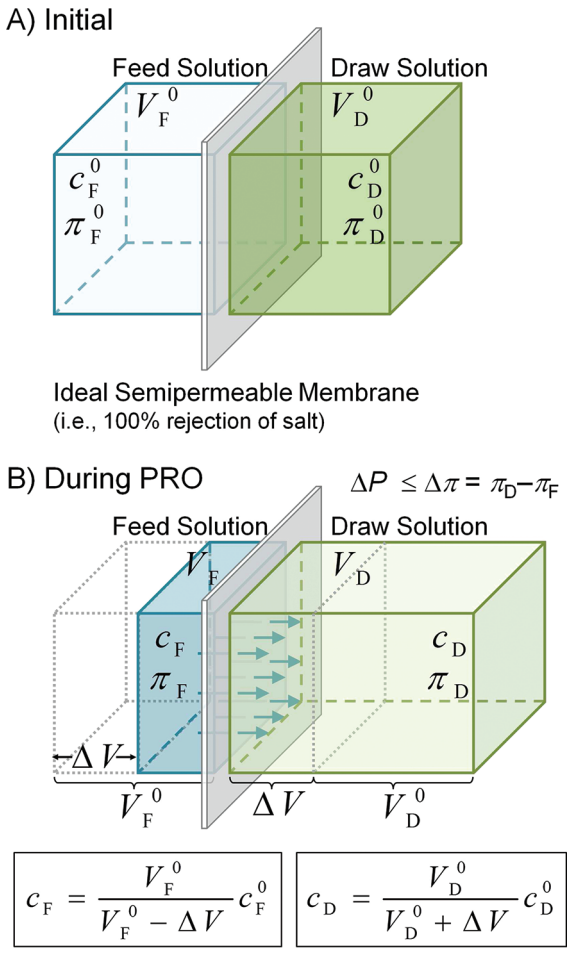

Figure 2. Schematics of a pressure retarded osmosis process. The draw and feed solutions are separated by an ideal semipermeable membrane that allows the passage of water while completely rejecting salt. (A) Initially, the higher concentration of the draw solution induces an osmotic pressure difference, $\Delta\pi = \pi_D^0 - \pi_F^0$, across the membrane to provide the driving force for water flux from the feed side to the draw side. (B) During the PRO process, the draw solution is pressurized by an applied hydraulic pressure, ΔP. Due to the cumulative volume of pure water, ΔV, that has permeated across the membrane, the feed solution is concentrated while the draw solution is diluted.

The difference in osmotic pressure drives water flux from the feed to the draw solution, as illustrated in Figure 2B. As water permeates across the membrane, it dilutes the draw solution to concentration $c_D = c_D^0 V_D^0/(V_D^0 + \Delta V)$, where ΔV is the permeate volume. Volume is conserved, based on the earlier assumption that the dilute solutions exhibit ideal behavior, and ΔV is equivalent to the increase in draw solution volume and decrease in feed solution volume. The concentration of the feed solution, hence, increases to $c_F = c_F^0 V_F^0/(V_F^0 - \Delta V)$ due to the complete rejection of salt by the membrane.

In the absence of an applied hydraulic pressure, water permeation is terminated when the concentrations of the draw and feed solutions equilibrate and the net osmotic driving force vanishes (i.e., $\Delta\pi = 0$). The concentration of the final solutions at this point, denoted by the superscript f, is

$$c_F^f = c_D^f = (1-\phi)c_D^0 + \phi c_F^0 \equiv c^f \tag{6}$$

where $\phi = V_F^0/(V_D^0 + V_F^0)$ is the ratio of the initial feed solution volume to both initial draw and feed solution volume. Note that ϕ is approximately the mole fraction because we assume the volumetric contribution of salt is negligible compared to that of water. Hence, ϕ is consistent with the previous definition used to determine the energy of mixing.

The total volume of permeate, ΔV^f, that ultimately passes into the draw solution can be calculated by solving ΔV for $c_D = c_F$:

$$\frac{\Delta V^f}{V_F^0} = \frac{1-\phi}{\phi}\left(\frac{c_D^0}{c^f} - 1\right) = \left(1 - \frac{c_F^0}{c^f}\right) \tag{7}$$

The final total permeate volume divided by the initial feed solution volume (eq 7) gives the fraction of V_F^0 that eventually permeates into the draw solution. SI Figure S1 shows $\Delta V^f/V_F^0$ as a function of ϕ for a river water or brackish water feed solution (1.5 and 17 mM NaCl, respectively) and a seawater draw solution (600 mM NaCl).

Reversible Thermodynamic PRO Process. In the theoretical reversible thermodynamic PRO model, an infinitesimal water flux is maintained throughout the osmosis process. This is achieved by applying a hydraulic pressure, ΔP, negligibly smaller than the osmotic pressure difference, $\Delta\pi$, on the draw solution such that an infinitesimally small volume of pure water permeates across the membrane. The draw solution is diluted very slightly by the minuscule permeate while the concentration of the feed solution increases a little. Hence, the osmotic pressure difference decreases such that $\Delta\pi = \Delta P$. The applied hydraulic pressure is then lowered marginally for another tiny drop of water to permeate across. Based on the van't Hoff relation, the osmotic pressure difference when ΔV has permeated across the membrane is linearly proportional to the concentration difference ($\Delta c = c_D - c_F$):

$$\Delta\pi = \nu RT\Delta c = \nu RT\left(\frac{V_D^0}{V_D^0 + \Delta V}c_D^0 - \frac{V_F^0}{V_F^0 - \Delta V}c_F^0\right) \tag{8}$$

The process of gradually reducing the applied hydraulic pressure is repeated in infinite small steps to achieve a continuous decrease in ΔP while keeping $\Delta P = \Delta\pi$. At any point during the process, the applied hydraulic pressure can be raised such that ΔP is just slightly higher than $\Delta\pi$. The process is thus "reversed" as an infinitesimally small volume of pure water permeates back into the feed solution. A representative plot of $\Delta\pi$ as a function of ΔV (eq 8) is shown in Figure 3A for a seawater draw solution and brackish water feed solution. The volumetric fraction of the feed solution $\phi = 0.4$ and $\nu = 2$ for NaCl. The horizontal axis intercept indicates the final permeate volume, ΔV^f, when the salinity difference reaches zero.

Substituting the initial draw solution volume expressed in terms of initial feed solution volume, $V_D^0 = (1-\phi)V_F^0/\phi$, into eq 8 yields

$$\Delta\pi = \nu RT\left(\frac{(1-\phi)c_D^0}{1-\phi\left(1-\frac{\Delta V}{V_F^0}\right)} - \frac{c_F^0}{1-\frac{\Delta V}{V_F^0}}\right) \tag{9}$$

Thus, using eq 9, we can express $\Delta\pi$ in terms of $\Delta V/V_F^0$—the volumetric fraction of the initial feed solution that has permeated into the draw solution. The osmotic pressure difference as a function of $\Delta V/V_F^0$ is shown in SI Figure S2 for a range of ϕ values with the same seawater draw solution and brackish water feed solution.

Theoretical Maximum Extractable Work is Equal to the Gibbs Energy of Mixing. In a reversible thermodynamic

dx.doi.org/10.1021/es300060m | Environ. Sci. Technol. 2012, 46, 5230−5239

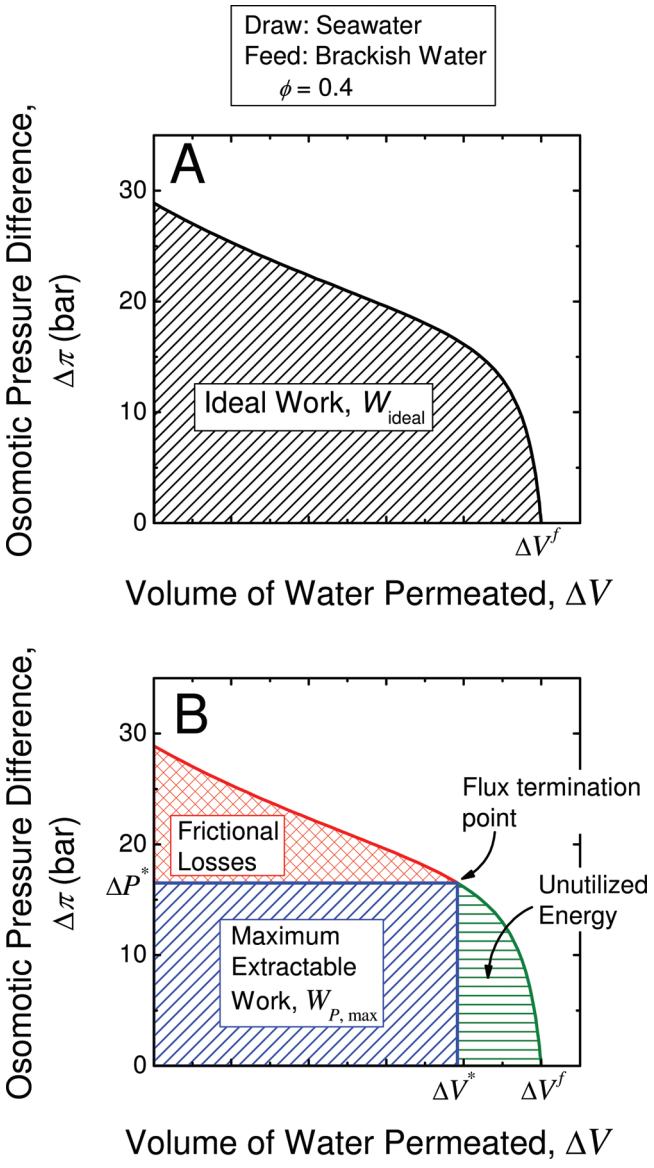

Figure 3. (A) Representative plot of the osmotic pressure difference between the draw and feed solution, $\Delta\pi$, as a function of the volume of water permeated, ΔV (eq 8), indicated by the solid black line. As water permeates across the membrane, the feed concentration increases while the draw concentration decreases. Therefore, $\Delta\pi$ decreases to zero as ΔV increases to ΔV^f (eq 7). In a reversible thermodynamic PRO process, the applied hydraulic pressure difference, ΔP, is always equal to $\Delta\pi$ to achieve an infinitesimal water flux; hence, the total amount of work extractable from the hypothetical PRO process, W_{ideal}, is equivalent to the area under the pressure−volume curve (eq 10). (B) Representative plot of the maximum amount of work that can be extracted in a constant-pressure PRO process, $W_{P,max}$. The area of the region marked "Frictional Losses" represents the energy required to overcome the frictional forces as water permeates across the semipermeable membrane. When $\Delta\pi = \Delta P^*$, the flux termination point is reached. The energy of mixing associated with the remaining volume of water that did not permeate across the membrane ($\Delta V^f - \Delta V^*$) is indicated by the region "Unutilized Energy". In these representative plots, the draw solution is seawater (600 mM or 35 g/L NaCl), the feed solution is brackish water (17 mM or 1000 mg/L NaCl), the volumetric fraction of the feed solution, ϕ, is 0.4, and temperature T = 298 K.

process, no entropy is generated.[15] Therefore, the work done by the expansion in volume of the pressurized draw solution in a reversible PRO process represents the ideal amount of work extractable. Integrating ΔP across the increase in draw solution volume (i.e., ΔV from 0 to ΔV^f) yields the maximum energy available for extraction—the ideal work, W_{ideal}:

$$W_{ideal} = \int_0^{\Delta V^f} \Delta P d(\Delta V) \tag{10}$$

A graphical representation of W_{ideal} is given by the area under the pressure−volume plot as depicted in Figure 3A.

As $\Delta P = \Delta\pi$ throughout reversible thermodynamic PRO, we can substitute eq 9 into eq 10 and solve the integral to arrive at the specific ideal work, W_{ideal,V_F^0}, defined as energy per unit volume of the initial feed solution:

$$-\frac{W_{ideal,V_F^0}}{\nu RT} = \frac{c^f}{\phi}\ln c^f - c_F^0 \ln c_F^0 - \frac{(1-\phi)}{\phi} c_D^0 \ln c_D^0 \tag{11}$$

The negative sign in eq 11 signifies that work is being done by the system. The specific ideal work is represented in SI Figure S2 as the area under the pressure−volume plots. An inspection of eq 11 shows that W_{ideal,V_F^0} is determined by the salt concentration, c^0, and relative proportion, ϕ, of the initial feed and draw solutions. More significantly, by comparing eq 11 with eq 5, we see that the theoretical maximum extractable work is equal to the Gibbs free energy of mixing. This is consistent with the principles of thermodynamics—the change in the Gibbs free energy of a system is equivalent to the work done by the system in an ideal reversible thermodynamic process.[15,16] Figure 1, therefore, also represents the ideal work extractable in a reversible PRO process.

ENERGY EFFICIENCY OF PRESSURE RETARDED OSMOSIS

Actual processes are not completely reversible in nature due to entropy production. Hence, the amount of energy that can be extracted will always be less than the theoretical maximum energy, W_{ideal}.[15] The second law of thermodynamics, therefore, imposes an upper limit on the efficiency that can be achieved by an actual energy extraction process such as PRO. In this section, we examine the thermodynamic efficiency of PRO power generation with natural salinity gradients, and discuss the inefficiencies intrinsic to the process.

Extractable Work in a Constant-Pressure PRO Process. In an actual PRO process, a constant hydraulic pressure is applied on the draw side, and the permeation of water ceases when $\Delta\pi$ is equal to the constant applied pressure. Therefore, the final total permeate volume is less than ΔV^f and is determined by substituting $\Delta\pi = \Delta P$ into eq 8. The work done by a constant-pressure PRO process (denoted by the subscript P) is the product of the applied pressure and the permeate volume:

$$W_P = \Delta P \Delta V = \nu RT\left(\frac{V_D^0}{V_D^0 + \Delta V} c_D^0 - \frac{V_F^0}{V_F^0 - \Delta V} c_F^0\right)\Delta V \tag{12}$$

As the final total permeate volume is a function of ΔP, W_P is dependent on the constant hydraulic pressure applied. Keeping the draw side highly pressurized would result in a small ΔV and a corresponding low W_P. Alternatively, a large permeate volume is achieved by maintaining a low ΔP, but the resultant W_P would consequently be small. Work is maximized when the constant-pressure PRO is operated at an optimum applied

dx.doi.org/10.1021/es300060m | Environ. Sci. Technol. 2012, 46, 5230−5239

hydraulic pressure, ΔP^*, and permeate volume, ΔV^*. Solving $dW_P/d\Delta P$ (or $dW_P/d\Delta V$) equal to zero yields

$$\Delta V^* = \frac{\sqrt{c_D^0} - \sqrt{c_F^0}}{\sqrt{c_D^0} + \frac{\phi}{1-\phi}\sqrt{c_F^0}} V_F^0 \quad (13)$$

$$\Delta P^* = \nu RT\left[(1-\phi)c_D^0 - \phi c_F^0 + (2\phi - 1)\sqrt{c_D^0 c_F^0}\right] \quad (14)$$

SI Figures S1 and S3 show $\Delta V^*/V_F^0$ (ratio of total permeation to initial feed solution volume) and ΔP^*, respectively, as a function of ϕ. Substituting eqs 13 and 14 into eq 12 gives the maximum extractable work in constant-pressure PRO, $W_{P,max}$:

$$W_{P,max} = \Delta P^* \Delta V^* = \nu RT(1-\phi)(\sqrt{c_D^0} - \sqrt{c_F^0})^2 V_F^0 \quad (15)$$

Figure 3B illustrates the optimum applied hydraulic pressure difference and permeate volume for a seawater draw solution and brackish water feed solution when $\phi = 0.4$. The maximum extractable work in constant pressure PRO is demarcated by the area of the patterned blue region. Dividing the maximum work by V_F^0 gives the specific $W_{P,max}$ (energy per unit initial feed solution volume). An examination of eq 15 reveals the constant negative slope of the function with respect to ϕ: $W_{P,max}$ is highest when ϕ is equal to zero, and as ϕ increases to one, the specific $W_{P,max}$ decreases linearly to zero.

Frictional Losses and Unutilized Energy. Because constant-pressure PRO is not a completely reversible process, $W_{P,max}$ is less than the ideal amount of work extractable (eq 11). During water permeation, the frictional forces between the water molecules and the membrane give rise to hydraulic resistance.[24,25] To achieve a nonzero water flux across the semipermeable membrane, a portion of the osmotic driving force is expended to overcome the resistance. Entropy is produced when energy is spent to counter the solvent−membrane friction. This energy is, thus, not tapped for useful work and is analogous to the irreversible energy loss in a reverse osmosis desalination process.[22,26] The energy attributed to frictional losses is represented as the area of the patterned red region in Figure 3B, and is expressed as

$$\text{Frictional Losses} = \int_0^{\Delta V^*} \Delta P d(\Delta V) - \Delta P^* \Delta V^* \quad (16)$$

In constant-pressure PRO, the actual permeate volume is smaller than the volume of water that would eventually permeate into an unpressurized draw solution. This is because the permeation of water is terminated when the osmotic pressure difference is equal to the constant applied hydraulic pressure (i.e., interception of horizontal line, ΔP, and $\Delta\pi$ curve in Figure 3B), before the feed and draw solutions reach the same concentration. At this point, the net driving force for water flux becomes zero. Hence, the energy of mixing embedded in the "unpermeated" volume ($\Delta V^f - \Delta V^*$) is not extracted for useful work. This "unutilized energy" is indicated as the area of green patterned region in Figure 3B, and is described by

$$\text{Unutilized Energy} = \int_{\Delta V^*}^{\Delta V^f} \Delta P d(\Delta V) \quad (17)$$

Thermodynamic Efficiency of PRO Work Extraction. The first law of thermodynamics stipulates that the sum of the useful, dissipated, and remaining energy (maximum extractable work, frictional losses, and unutilized energy, respectively) is equal to the ideal work.[15,16] Figure 4 (top) shows stacked plots of the specific energies as a function of ϕ, for river water (A) and brackish water (B) feed solution. The wedges representing frictional losses and unutilized energy (patterned red and green region, respectively) are stacked on top of the specific $W_{P,max}$ (patterned blue region) to yield the specific ideal work, W_{ideal,V_F^0}. Adding up the specific energies in these plots yields the specific Gibbs free energy of mixing, $\Delta G_{mix,V_A}$, indicated in Figure 1 (solid blue line and dashed red line for a river water and brackish water feed solution, respectively).

The thermodynamic efficiency of work extraction, η, is defined as the maximum percent of the Gibbs free energy of mixing, or ideal work, that can be extracted in constant-pressure PRO:

$$\eta = \frac{W_{P,max}}{\Delta G_{mix}} \times 100\% \quad (18)$$

The thermodynamic efficiency is calculated by substituting eqs 5 (or 11) and 15 into eq 18. Here, we assume zero energy losses from the PRO system components, such as pumps, pressure exchangers, and hydroturbines. Hence, η represents the thermodynamic limit of work extraction and is a measure of the inefficiencies due to entropy production and unutilized energy that are intrinsic to constant-pressure PRO. An inspection of eqs 5 (or 11) and 15 reveals that η is determined by the initial salt concentrations and relative proportion, ϕ, of the feed and draw solutions. Figure 4 (bottom) shows η (solid blue line) for a river water (A) and brackish water (B) feed solution paired with a seawater draw solution. The portion of energy consumed by frictional losses and the unutilized energy of mixing are indicated by the dashed red line and dotted green line, respectively.

For a river water−seawater PRO system, the specific $W_{P,max}$ is largest at 0.75 kWh/m^3 (2.68 kJ/L) when $\phi = 0$, and decreases linearly to zero as ϕ increases to unity (eq 15 and Figure 4A, top). The thermodynamic efficiency decreases concomitantly from 91.1 to 18.1% (Figure 4A, bottom). Therefore, it is energetically desirable to operate constant-pressure PRO at small ϕ values (i.e., small feed solution volume is paired with a large draw solution volume) to simultaneously achieve a high specific $W_{P,max}$ and η. In an actual crossflow membrane module, ϕ is determined by the volumetric flow rate in the feed and draw channels. Hence, a small ϕ corresponds to a relatively low feed stream flow rate. A similar trend is observed for the brackish water−seawater system (Figure 4B): the specific $W_{P,max}$ and η are highest at 0.57 kWh/m^3 (2.06 kJ/L) and 79.4%, respectively, when ϕ approaches zero. The lower salt concentration in the initial river water feed solution, relative to the brackish water, allows a higher specific $W_{P,max}$ and thermodynamic efficiency to be attained. However, the higher purity of river water also signifies that it is a more precious and desirable resource compared to brackish water. These, and other, factors will need to be considered when selecting the feed solution for PRO power generation with natural salinity gradients.

Practical Constraints in PRO Operation. Membrane power density (power produced per membrane area) is a key factor in determining the economical feasibility of PRO power generation.[3,9,27] Operating at a high power density will maximize the utilization of membrane area, thereby reducing capital cost and enhancing cost-effectiveness.[3,9] To maximize power

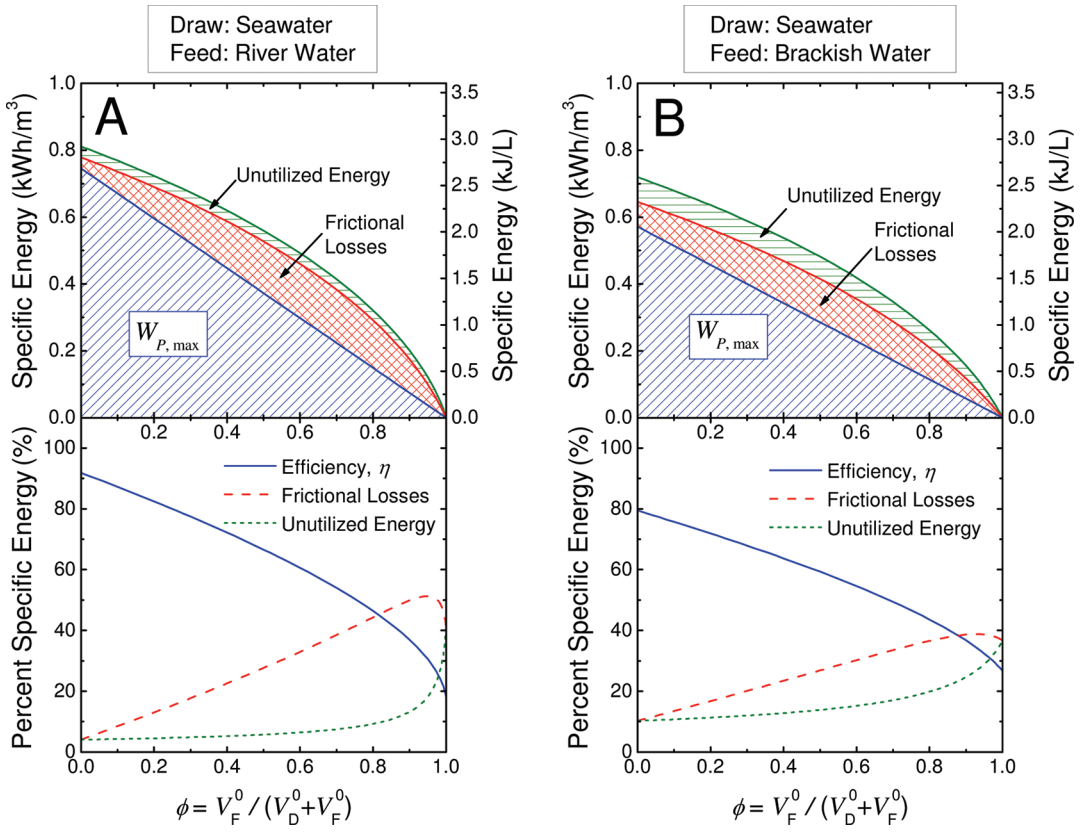

Figure 4. Top: Specific maximum extractable work, frictional losses, and unutilized energy in a constant-pressure PRO process as a function of the volumetric fraction of feed solution to both draw and feed solutions, ϕ. Bottom: Efficiency of work extraction (solid blue line), defined as the percent of total free energy of mixing that is extractable in a constant-pressure PRO process, as a function of ϕ. The percent of energy required to overcome the frictional forces as water is driven across the semipermeable membrane (i.e., frictional losses) is indicated by the dashed red line. The dotted green line represents the percent of total energy that is unutilized due to the osmotic pressure difference being smaller than the constant applied hydraulic pressure difference (i.e., $\Delta\pi \leq \Delta P$). (A) River water (1.5 mM NaCl) and (B) brackish water (17 mM NaCl) are employed as the feed solutions. The draw solution is seawater (600 mM NaCl) and temperature T = 298 K.

density, a hydraulic pressure approximately half of the osmotic pressure difference is applied across the membrane, i.e., $\Delta P \approx (\pi_D - \pi_F)/2$.[10,27] However, based on our preceding discussion, the ΔP requirement for maximum power density is incompatible with the condition for achieving maximum extractable work in constant-pressure PRO, $W_{P,\max}$ (eq 15). Therefore, when PRO is operated to maximize power density, the extractable work is not fully accessed (except for ϕ = 0.5, where both aims are simultaneously realized).

Membrane power density is the product of the PRO water flux and the applied hydraulic pressure,[27] while the water flux is proportional to the effective osmotic driving force across the membrane.[27,28] As PRO progresses, the osmotic driving force ($\Delta\pi - \Delta P$) decreases due to dilution of the draw solution and concentration of the feed solution. Beyond a certain point, the ensuing water flux and power density become too low for cost-effective operation. The practical constraint to sustain an appreciable water flux at all points along the membrane requires the process to be terminated before the effective driving force reaches zero. Hence, the actual permeate volume, ΔV_{actual}, is lower than the total volume that would eventually permeate if the process had proceeded to completion.

A representation of the two operational constraints on work extraction is depicted in Figure 5 for a brackish water−seawater PRO system with ϕ = 0.4. The process is operated at a constant-pressure of $\Delta P_{actual} = (\pi_D^0 - \pi_F^0)/2$ (14.5 bar) to maximize membrane power density.[10,27] When the effective osmotic driving force falls below a certain level, the process is discontinued. The actual extractable work, $W_{P,actual}$, frictional losses, and unutilized energy are represented by the areas of patterned blue, red, and green regions, respectively. To facilitate comparison, the maximum extractable work, $W_{P,max}$, is indicated by the area within the dashed blue line.

To maximize power density, the required applied hydraulic pressure departs from the optimal ΔP^* and the actual extractable work is lower than $W_{P,max}$. Figure 5 shows that more energy is expended to overcome membrane hydraulic resistance and achieve a higher water flux (indicated by the overlapped area of $W_{P,max}$ and frictional losses). That is, work is consumed for entropy production instead. As PRO proceeds, the dwindling water flux causes the membrane power density to diminish and eventually triggers the process to be discontinued. The remaining energy of mixing is unutilized and, therefore, a greater portion of the available energy is not extracted for power generation (area of patterned green region in Figure 5).

The operational objectives to maximize and maintain sufficient power density are not aligned with the goal of maximum work extraction. In satisfying the practical power density requirements, the maximum extractable work in constant-pressure PRO is not fully exploited. The actual efficiency of PRO work extraction, $\eta_{actual} = (W_{P,actual}/\Delta G_{mix}) \times 100\%$ is lower than the constant-pressure thermodynamic efficiency, i.e., $\eta_{actual} < \eta$. Therefore, practical PRO systems will need to balance the two inconsistent objectives of maximizing power

dx.doi.org/10.1021/es300060m | Environ. Sci. Technol. 2012, 46, 5230−5239

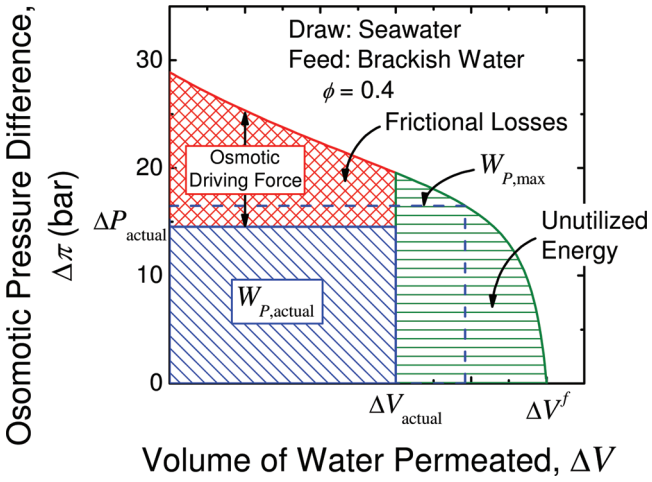

Figure 5. Representative plot of the amount of work that can be extracted in an actual constant-pressure PRO process, $W_{P,actual}$. The osmotic pressure difference in excess of the hydraulic pressure (i.e., $\Delta\pi - \Delta P$) provides the driving force for water flux (i.e., to overcome frictional losses). In an actual PRO process, the constant applied hydraulic pressure difference is constrained by the operational need to sustain sufficient water flux. Therefore, the actual work that is extracted, represented by the patterned region marked $W_{P,actual}$, is less than the $W_{P,max}$, indicated by area under the dotted blue line. In this representative plot, the draw solution is seawater (600 mM NaCl), the feed solution is brackish water (17 mM NaCl), the volumetric fraction of the feed solution, ϕ, is 0.4, and the temperature T = 298 K.

density and maximizing extraction efficiency through the operating parameters (applied hydraulic pressure and process termination point).

IMPLICATIONS FOR PRO ENERGY PRODUCTION

Our recent studies demonstrated the intricate influence of membrane properties on PRO power density performance.[10,11] The membrane transport and structural parameters relate the bulk osmotic pressure difference and applied hydraulic pressure to the power density.[10,11,27] A higher power density can be attained under the same operating conditions by employing high performance membranes—active layer with high water permeability and salt selectivity, coupled with customized support layer that suppresses the detrimental effect of internal concentration polarization.[10,11] Improved membranes can enable PRO to be operated cost-effectively even when power density is not maximized, i.e., $\Delta P_{actual} \neq (\pi_D - \pi_F)/2$. Higher performance membranes will also better utilize small osmotic pressure differences to produce relatively higher water fluxes, thereby enabling the generation of adequate power densities even with the dwindled $\Delta\pi$ toward the later phase of the PRO process. As the process is allowed to proceed further, a larger portion of the free energy of mixing is converted to usable work. Therefore, the innovation of PRO membranes with the desired transport and structural properties can enhance the efficiency of work extraction while maintaining sufficient water flux and power density for cost-effective operation.

Fouling is a key issue affecting productivity in membrane processes as it gives rise to flux decline and shortened membrane life-span.[22,29−31] To mitigate these detrimental effects, pretreatment of the input streams is typically employed in separation processes, such as reverse osmosis desalination, which incurs an additional energy cost to the overall process.[22,29,31,32] The PRO input feed stream will similarly need to undergo pretreatment to control membrane fouling.[33] Here, brackish water can have an advantage over river water. Brackish waters from groundwater are naturally filtered through the subsurface. Hence, a significant portion of the organic and colloidal matter that causes membrane fouling is naturally removed.[34] Employing brackish groundwater with lower fouling potential, instead of surface river water, can potentially reduce the energy requirement for pretreatment, thus making PRO power generation from salinity gradients more attractive.

Technological advances that are within our reach can address some of the above-mentioned challenges. If the obstacles are adequately overcome, PRO can potentially harvest part of the energy of mixing from the annual global river discharge of ~37 300 km^3 to generate a significant source of clean sustainable energy.[4] For a PRO power plant operated at an actual efficiency η_{actual} = 60% with a river water feed solution and a seawater draw solution, i.e., ΔG_{mix} = 0.77 kWh/m^3, the specific extractable work will be $\eta_{actual} \times \Delta G_{mix}$ = 0.46 kWh/m^3. Assuming a further 20% is lost from inefficiencies in PRO system components, 0.37 kWh of useful work can be derived per cubic meter of the river water feed solution.

Channeling a tenth of the global river water discharge (i.e., 3730 km^3/y) for PRO can potentially generate 157 GW of renewable power, or 1370 TWh/y, after factoring in the conservative estimations on process losses and inefficiencies. This is equivalent to the electrical consumption of 520 million people, based on the average global electricity use of ~300 W/capita.[35] Producing the same amount of electricity through coal-fired power plants, which release 1 kg of CO_2 equivalent per kWh generated,[36] would emit ~1.37 × 10^9 metric tons of greenhouse gases in CO_2 equivalent. Nature's hydrological cycle offers a significant source of sustainable energy through salinity gradients. Further studies to better our understanding of the technology will enable the realization of these clean and renewable power sources toward alleviating our current climate change and energy issues.

ASSOCIATED CONTENT

Supporting Information

Presentation of the energy change of mixing for a binary system of aqueous strong electrolyte solutions; summary of the Gibbs free energy of mixing with, and without, the activity coefficient (Table S1); summary of sodium chloride activity coefficients at different molar concentrations (Table S2); plot of fraction of initial feed solution volume that permeates into the draw solution, as a function of the volumetric fraction of the feed solution (Figure S1); plot of osmotic pressure difference between the draw and feed solutions, as a function of the volumetric fraction of initial feed solution permeated (Figure S2); plot of applied hydraulic pressure difference in order to maximize the work that can be extracted in a constant pressure PRO process, as a function of the volumetric fraction of the feed solution (Figure S3). This information is available free of charge via the Internet at http://pubs.acs.org/ .

AUTHOR INFORMATION

Corresponding Author

*E-mail: menachem.elimelech@yale.edu; phone: (203) 432-2789.

Notes

The authors declare no competing financial interest.

■ ACKNOWLEDGMENTS

We acknowledge the Graduate Fellowship (to N.Y.Y.) made by the Environment and Water Industrial Development Council of Singapore.

■ NOMENCLATURE

c	molar concentration
Δc	salt concentration difference across the membrane
G	molar Gibbs free energy of solution
ΔG_{mix}	molar Gibbs free energy of mixing
$\Delta G_{mix,V_A}$	specific Gibbs free energy of mixing
$\Delta G_{mix,V_M}$	Gibbs free energy of mixing per unit volume of the resultant mixture
N	number of moles in solution
ΔP	applied hydraulic pressure difference across the membrane
R	gas constant
T	absolute temperature
V	volume of solution
ΔV	permeate volume
x_i	mole fraction of species i in solution
W_{ideal}	ideal work
W_{ideal,V_F^0}	specific ideal work
W_P	work done by a constant-pressure PRO process
$W_{P,max}$	maximum work done by a constant-pressure PRO process

■ GREEK SYMBOLS

γ_i	activity coefficient of species i
η	thermodynamic efficiency
η_{actual}	work extraction efficiency in an actual PRO process
ν	number of ions each electrolyte molecule dissociates into
π	osmotic pressure of the solution
$\Delta\pi$	osmotic pressure difference across the membrane
ϕ	ratio of total moles (or volume) of the solution to total moles (or volume) of the system

■ SUPERSCRIPTS

0	initial
f	final
*	optimum parameter to achieve maximum work in a constant-pressure PRO process

■ SUBSCRIPTS

A	solution A
B	solution B
D	draw solution
F	feed solution
M	resultant mixture
s	salt species
w	water species

■ REFERENCES

(1) Hoffert, M. I.; Caldeira, K.; Benford, G.; Criswell, D. R.; Green, C.; Herzog, H.; Jain, A. K.; Kheshgi, H. S.; Lackner, K. S.; Lewis, J. S.; Lightfoot, H. D.; Manheimer, W.; Mankins, J. C.; Mauel, M. E.; Perkins, L. J.; Schlesinger, M. E.; Volk, T.; Wigley, T. M. L. Advanced technology paths to global climate stability: Energy for a greenhouse planet. *Science* **2002**, *298* (5595), 981−987.

(2) Pattle, R. E. Production of Electric Power by Mixing Fresh and Salt Water in the Hydroelectric Pile. *Nature* **1954**, *174* (4431), 660−660.

(3) Ramon, G. Z.; Feinberg, B. J.; Hoek, E. M. V. Membrane-based production of salinity-gradient power. *Energy Environ. Sci.* **2011**, *4* (11), 4423−4434.

(4) Dai, A.; Trenberth, K. E. Estimates of freshwater discharge from continents: Latitudinal and seasonal variations. *J. Hydrometeorol.* **2002**, *3* (6), 660−687.

(5) La Mantia, F.; Cui, Y.; Pasta, M.; Deshazer, H. D.; Logan, B. E. Batteries for Efficient Energy Extraction from a Water Salinity Difference. *Nano Lett.* **2011**, *11* (4), 1810−1813.

(6) Lacey, R. E. Energy by reverse electrodialysis. *Ocean Eng.* **1980**, *7* (1), 1−47.

(7) Post, J. W.; Hamelers, H. V. M; Buisman, C. J. N. Energy Recovery from Controlled Mixing Salt and Fresh Water with a Reverse Electrodialysis System. *Environ. Sci. Technol.* **2008**, *42* (15), 5785−5790.

(8) Loeb, S. Osmotic Power-Plants. *Science* **1975**, *189* (4203), 654−655.

(9) Achilli, A.; Childress, A. E. Pressure retarded osmosis: From the vision of Sidney Loeb to the first prototype installation - Review. *Desalination* **2010**, *261* (3), 205−211.

(10) Yip, N. Y.; Tiraferri, A.; Phillip, W. A.; Schiffrnan, J. D.; Hoover, L. A.; Kim, Y. C.; Elimelech, M. Thin-Film Composite Pressure Retarded Osmosis Membranes for Sustainable Power Generation from Salinity Gradients. *Environ. Sci. Technol.* **2011**, *45* (10), 4360−4369.

(11) Yip, N. Y.; Elimelech, M. Performance Limiting Effects in Power Generation from Salinity Gradients by Pressure Retarded Osmosis. *Environ. Sci. Technol.* **2011**, *45* (23), 10273−10282.

(12) Chou, S.; Wang, R.; Shi, L.; She, Q.; Tang, C.; Fane, A. G. Thin-film composite hollow fiber membranes for pressure retarded osmosis (PRO) process with high power density. *J. Membr. Sci.* **2012**, *389*, 25−33.

(13) Thorsen, T.; Holt, T. The potential for power production from salinity gradients by pressure retarded osmosis. *J. Membr. Sci.* **2009**, *335* (1−2), 103−110.

(14) Nijmeijer, K.; Metz, S.; Isabel, C. E.; Andrea, I. S. f. Chapter 5. Salinity Gradient Energy. In *Sustainability Science and Engineering*; Elsevier; Vol. *2*, pp 95−139.

(15) Smith, J. M.; Van Ness, H. C.; Abbott, M. M. *Introduction to Chemical Engineering Thermodynamics*, 7th ed.; McGraw-Hill: Boston, MA, 2005; p xviii, 817 pp.

(16) Sandler, S. I. *Chemical and Engineering Thermodynamics*, 3rd ed.; Wiley: New York, 1999; p xx, 772 pp.

(17) Mistry, K. H.; McGovern, R. K.; Thiel, G. P.; Summers, E. K.; Zubair, S. M.; Lienhard, J. H. Entropy Generation Analysis of Desalination Technologies. *Entropy* **2011**, *13* (10), 1829−1864.

(18) Robinson, R. A. Stokes, R. H. *Electrolyte Solutions*, 2nd rev. ed.; Dover Publications: Mineola, NY, 2002; p xv, 571 pp.

(19) King, C. J. *Separation Processes*, 2d ed.; McGraw-HillL New York, 1980; p xxvi, 850 pp.

(20) Pitzer, K. S.; Peiper, J. C.; Busey, R. H. Thermodynamic Properties of Aqueous Sodium-Chloride Solutions. *J. Phys. Chem. Ref. Data* **1984**, *13* (1), 1−102.

(21) Semiat, R. Energy Issues in Desalination Processes. *Environ. Sci. Technol.* **2008**, *42* (22), 8193−8201.

(22) Elimelech, M.; Phillip, W. A. The Future of Seawater Desalination: Energy, Technology, and the Environment. *Science* **2011**, *333* (6043), 712−717.

(23) Morel, F. Hering, J. G. *Principles and Applications of Aquatic Chemistry*; Wiley: New York, 1993; p xv, 588 pp.

(24) Kedem, O.; Katchalsky, A. Thermodynamic Analysis of the Permeability of Biological Membranes to Non-Electrolytes. *Biochim. Biophys. Acta* **1958**, *27* (2), 229−246.

(25) Spiegler, K. S.; Kedem, O. Thermodynamics of hyperfiltration (reverse-osmosis) - criteria for efficient membranes. *Desalination* **1966**, *1* (4), 311−326.

(26) Liu, C.; Rainwater, K.; Song, L. F. Energy analysis and efficiency assessment of reverse osmosis desalination process. *Desalination* **2011**, *276* (1−3), 352−358.

(27) Lee, K. L.; Baker, R. W.; Lonsdale, H. K. Membranes for Power-Generation by Pressure-Retarded Osmosis. *J. Membr. Sci.* **1981**, *8* (2), 141−171.
(28) Mehta, G. D.; Loeb, S. Internal Polarization in the Porous Substructure of a Semipermeable Membrane under Pressure-Retarded Osmosis. *J. Membr. Sci.* **1978**, *4* (2), 261−265.
(29) Baker, R. W. *Membrane Technology and Applications*, 2nd ed.; J. Wiley: Chichester; New York. 2004; p x, 538 pp.
(30) Mi, B.; Elimelech, M. Chemical and physical aspects of organic fouling of forward osmosis membranes. *J. Membr. Sci.* **2008**, *320* (1−2), 292−302.
(31) National Research Council. *Desalination: A National Perspective*; The National Academies Press, 2008; p 312.
(32) Fritzmann, C.; Lowenberg, J.; Wintgens, T.; Melin, T. State-of-the-art of reverse osmosis desalination. *Desalination* **2007**, *216* (1−3), 1−76.
(33) Loeb, S. Production of Energy from Concentrated Brines by Pressure-Retarded Osmosis: I. Preliminary Technical and Economic Correlations. *J. Membr. Sci.* **1976**, *1* (1), 49−63.
(34) Greenlee, L. F.; Lawler, D. F.; Freeman, B. D.; Marrot, B.; Moulin, P. Reverse osmosis desalination: Water sources, technology, and today's challenges. *Water Res.* **2009**, *43* (9), 2317−2348.
(35) EIA. International Energy Data and Analysis. http://www.eia.doe.gov/international/.
(36) Evans, A.; Strezov, V.; Evans, T. J. Assessment of sustainability indicators for renewable energy technologies. *Renew. Sustain. Energy Rev.* **2009**, *13* (5), 1082−1088.